Investigation of Impinging-Jet Crystallization with a Calcium Oxalate Model System

Jean M. Hacherl, Edward L. Paul, and Helen M. Buettner
Dept. of Chemical & Biochemical Engineering, Rutgers, The State University of New Jersey, 98 Brett Road, Piscataway, NJ 08854

An impinging-jet crystallizer was investigated in this work to assess its operational sensitivity and reproducibility for the production of small, monodisperse crystals using calcium oxalate, a model system capable of forming multiple hydrates. The impinging-jet mixer provides rapid mixing of the reactant solutions through the impingement of two narrow reactant streams at high velocity. Impinging jet linear velocity and postjetting conditions were studied, with the jet operated in nonsubmerged mode. Hydrate form and crystal-size distribution (CSD) were determined using optical microscopy and image analysis techniques. The impinging jet consistently produced small, monodisperse crystals. However, at a high level of supersaturation, slight variations in the CSD were observed for apparently identical conditions, suggesting a degree of sensitivity in the system that could lead to difficulty in its application. An apparent trend between impinging-jet linear velocity and crystal size and number was observed, with more small crystals produced at higher linear velocity.

Introduction

Over 90% of all pharmaceutical products contain drugs in particle, generally crystalline form. Crystallization determines drug chemical purity and physical properties including particle habit and size, crystal structure, and degree of crystal imperfection (Garside, 1991). The control and operation of crystallization processes is among the most important challenges in pharmaceutical development from both an industrial and a regulatory viewpoint (Shekunov and York, 2000). The crystal-size distribution (CSD) is a critical property, affecting drug bioavailability stability, and postcrystallization processing. Small, monodisperse crystals with a high surface area are often desired for increased bioavailability but can be difficult to produce because such crystals are generally formed by mixing two reactants to create a highly supersaturated environment in which nucleation tends to be a rapid process. Achieving uniform mixing prior to crystal nucleation requires faster mixing than is typically possible in conventional crystallizers. The presence of concentration gradients during crystal formation can lead to a wide CSD (Dirksen and Ring, 1991). The impinging-jet mixer is a device in which rapid mixing is achieved by the impingement of two high-velocity reactant streams, potentially generating rapid crystallization in the absence of concentration gradients and leading to a monodisperse population of small, high surface area crystals.

Crystallization consists of two steps: (1) nucleation, a preorganizing of the solute in the solution to obtain clusters (Mersmann, 1995), which if large enough create a stable nuclei, and (2) the subsequent growth of the nuclei. Both nucleation and growth are dependent on supersaturation; the nucleation rate increases exponentially with increasing supersaturation, while the growth rate increases linearly. At low supersaturation, the crystal size is controlled by the growth process. Once a critical supersaturation level, the metastable limit is reached, the nucleation rate increases rapidly and, as a result, a large number of crystals with a smaller average size is produced (Nyvlt, 1971). The high levels of supersaturation required for a nucleation-dominated process are usually achieved by reaction or antisolvent crystallization, in which two reactant streams are mixed to create a supersaturated environment. In these environments, the nucleation process

Correspondence concerning this article should be addressed to H. M. Buettner.
E. L. Paul is retired from Merck & Co., Inc.
Current address of J. M. Hacherl, Merck & Co., Inc., P.O. Box 4, WP97-B220, West Point, PA 19486.

can be extremely fast, requiring rapid mixing to eliminate concentration gradients. In slow, growth controlled crystallization, mixing is not as critical; however, slow crystallization generally results in large, lower surface area crystals that require milling to meet size or monodispersity requirements. Milling is undesirable because of yield losses, potential personnel exposure to chemically potent pharmaceutical compounds, and because mechanical stresses can reduce the stability of some pharmaceutical products (Midler et al., 1994) or introduce polymorphic modifications and transformation (Shekunov and York, 2000).

In cases where very small crystals are required for bioavailability and/or when milling is not an option, a nucleation-dominated process is desired. For example, inhalation delivery systems, which typically consist of crystalline particles in the form of drug/excipient mixtures or particle suspension, require small, monodisperse crystals (Shekunov and York, 2000). Only particles of a dia. less than 5 μm are able to reach the deep lung region containing the majority of blood vessels, which is the target for drug delivery. Further constraints are put on the CSD, because submicron particles are likely to be exhaled, necessitating a narrow CSD between 1 and 5 μm for efficient drug delivery. The difficulty with a nucleation-dominated process is that fast mixing is critical to ensure a homogeneous environment prior to the onset of nucleation. In a typical stirred-tank vessel the reaction rates can vary significantly throughout the reactor due to inhomogeneities in reactant concentration (Liszi et al., 1997; Van Leeuwen et al., 1996). An inhomogeneous field of supersaturation in a precipitator causes different driving forces for crystal growth and nucleation, leading to a nonuniform crystal product (Manth et al., 1996; Franke and Mersmann, 1995).

The system examined in this article, the impinging-jet mixer, has been shown to produce a well-mixed environment suitable for rapid nucleation and crystal growth. The two-impinging-jet mixer (TIJ) was first developed for rapid crystallization of pharmaceutical compounds at Merck & Co. (Midler et al., 1994). The impinging-jet system provides rapid micromixing of reactant solutions through the impingement of two narrow reactant streams at high velocity. In principle, a homogeneous environment is created in the impinging jet prior to nucleation, allowing rapid precipitation in the absence of concentration gradients, leading to a monodisperse, high surface area population of crystals. Mahajan and Kirwan (1996) used the two-step Bourne reaction between 1-naphthol and diazosulfanilic acid to develop a relationship for the characteristic mixing time as a function of jet diameter and Reynolds number. The authors found that the mixing time in the jet was at least as small as 65 ms. Using the pharmaceutical compound, Lovastatin, the authors also demonstrated that the CSD was only affected by micromixing when the time constant for micromixing was comparable to or larger than the nucleation induction time. Schaer et al. (1999) also used a system of parallel competing reactions to characterize micromixing intensity in a TIJ mixer immersed in a stirred-tank reactor. The authors found that the characteristic time for mixing decreased with increasing feed flow rate and reached values as small as 4 ms for jet velocities greater than 5 m/s. At jet velocities greater than 3 m/s, the impeller speed had a negligible effect and micromixing was controlled entirely by the impinging jets. In a similar system, Benet et al. (1999) found that at high supersaturation both nucleation and growth of barium sulphate could be completed in the TIJ mixer zone; external stirring had no effect on the CSD. They also found that the jet velocity had no significant effect on the CSD in the range of 5–20 m/s. This result contrasts with that of Mahajan and Kirwan (1996), who observed a dependence of CSD on jet velocity in this range. The CSD is expected to be dependent on jet velocity if the mixing time is of the same order of magnitude or slower than the reaction time. The results of Benet et al. (1999) suggest that the mixing time in their system was always faster than the reaction time in the jet velocity range of 5–20 m/s.

In addition to controlling the CSD, the level of supersaturation at which crystallization occurs also determines possible crystalline forms and transformations (Garside, 1991). Precipitated products can often be produced in a variety of forms, such as different polymorphs, hydrates, solvates, or amorphous phases (Rodriguez-Hornedo and Murphy, 1999; Dunitz and Bernstein, 1995; McCauley, 1991). Normally, only one of the possible forms has the desired product properties, making control of crystal form vital to product quality. In many cases, particularly when the supersaturation is high (the solution is far from the equilibrium concentration), kinetic considerations dominate and thermodynamically metastable phases are produced. These unstable phases may subsequently transform to other metastable phases or to the equilibrium form (Garside, 1991).

Calcium oxalate represents a useful model system for studying pharmaceutical compounds because, like most pharmaceutical compounds, it has rapid precipitation kinetics. Calcium oxalate precipitates from solution as one or more of three different hydrates depending on pH, temperature, supersaturation, calcium-to-oxalate ratio, and hydrodynamics. The thermodynamically stable calcium oxalate monohydrate

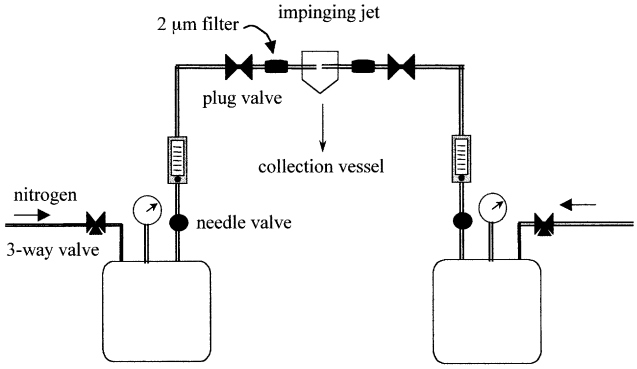

Figure 1. The bench-scale impinging-jet system used for calcium oxalate crystallization experiments consisted of the impinging jet, two 4-L stainless steel reservoir vessels for the reactant solutions, and the associated tubing and valves to control the flow to the jet chamber.

The impinging jet itself consisted of a glass chamber housing a stainless steel nozzle apparatus with two 1-mm nozzles. The reservoir vessels were pressurized with nitrogen gas to transport the reactants through tubing to the impinging jet. The reactants were filtered through in-line, 2-μm Teflon filters just prior to entering the impinging-jet mixer.

and the metastable dihydrate occur naturally in plant tissues, urinary calculi, and sediments of biological origin (Skrtic et al., 1984; Finlayson, 1978). Calcium oxalate trihydrate is the least stable of the three hydrates, and may be a precursor in urinary stone formation (Bretherton and Rodgers, 1998). The appearance of metastable phases is frequently encountered at high supersaturation, making precipitation processes prone to the formation of such phases (Brecevic et al., 1986).

This article explores the operational sensitivity and reproducibility of an impinging-jet mixer operated in the nonsubmerged mode to produce small monodisperse crystals. In particular, we examine the variability of the CSD and the hydrate distribution.

Materials and Methods

The bench-scale impinging-jet system used in this work (Figure 1) was modeled after the work of Mahajan and Kirwan (1996). The jet consisted of a glass chamber housing a stainless steel nozzle apparatus with two 1-mm nozzles. The glass chamber was large enough to prevent liquid buildup, allowing the streams to impinge directly without passing through liquid. In addition to the jet itself, the system consisted of two 4-L stainless steel reservoir vessels (Pope Scientific, Englewood, NJ) for the reactant solutions. The vessels were pressurized with nitrogen gas to transport the liquids through stainless steel tubing to the impinging jet. In-line rotameters were used to indicate the liquid flow rates to the impinging jet. A needle valve before each rotameter was used to regulate flow and a plug valve after each was used as an on/off switch. Each solution was filtered through an in-line 2-μm Teflon filter (Cole-Parmer, Vernon Hills, IL) just before entering the impinging-jet mixer.

Calcium chloride ($CaCl_2$-$2H_2O$, Fisher Scientific, Pittsburgh, PA) and sodium oxalate ($Na_2C_2O_4$, Fisher Scientific) were dissolved in deionized, distilled water to prepare the reactant solutions. The experiments were performed with equimolar $CaCl_2$ and $Na_2C_2O_4$ solutions adjusted to ionic strength 0.2 M with NaCl (Fisher Scientific) and pH adjusted to 6.5. Experiments were performed at room temperature (23–24°C). The jetted samples were either collected into a just-saturated calcium oxalate quench solution (quenched samples) or into an empty flask (unquenched samples). To prepare the quench solution, an excess of calcium oxalate (CaC_2O_4-H_2O, Fisher Scientific) was dissolved in deionized, distilled water and the ionic strength was adjusted to 0.2 M with NaCl. The solution was stirred overnight, filtered through a 0.2-μm filter (Fisher Scientific), and adjusted to a pH of 6.5. For the quenched samples, a 150-mL sample was collected directly into 500 mL of saturated calcium oxalate quench solution. In experiments performed with 5.0-mM reactant solutions, a second 20-mL sample was collected into a syringe for calcium analysis. Silicone tubing (3/16 in.) connected to the impinging-jet outlet was used to transfer the jetted material into the quench solution. The outlet tubing length was adjusted to maintain a residence time of 5–6 s for the different linear velocities investigated. The calcium oxalate quench solution was mixed continuously with a mechanical flat-blade agitator. Samples were taken from either the quenched solution or the empty flask 3 min after the completion of jetting. The 1-mL samples were placed into 35-mm glass-bottom microwell dishes (MatTek, Ashland, MA) and allowed to settle for 30 min prior to imaging. The 20-mL sample taken for calcium measurement was immediately filtered through a 0.2 μm syringe filter and analyzed using a calcium titration kit (Chemetrics, Calvern, VA). The sample was filtered to remove any crystals that had already formed, halting further growth that would reduce the amount of calcium in solution.

The samples taken from the quenched solution were imaged with a confocal microscope operated in transmitted light mode using a 40× objective lens with a 2× zoom. A macro was used to move the programmable microscope stage in a 5×5 block of 160-μm increments and capture and store the image at each position. Each 5×5 block of images took approximately 3 min to image. Generally, four blocks of images (100 images) were taken within a 20-min time period. The stored images were analyzed using Image-Pro Plus software (Media Cybernetics, Silver Spring, MD). A macro program written with Image-Pro Plus was used to count and size the crystals. A manual tagging option in the software was used to label the different calcium oxalate hydrate forms, allowing hydrate distributions to be determined. Two calcium oxalate hydrate forms were observed in this work: calcium oxalate monohydrate, which appeared in two shapes, designated COM1 and COM2, and calcium oxalate dihydrate (COD;

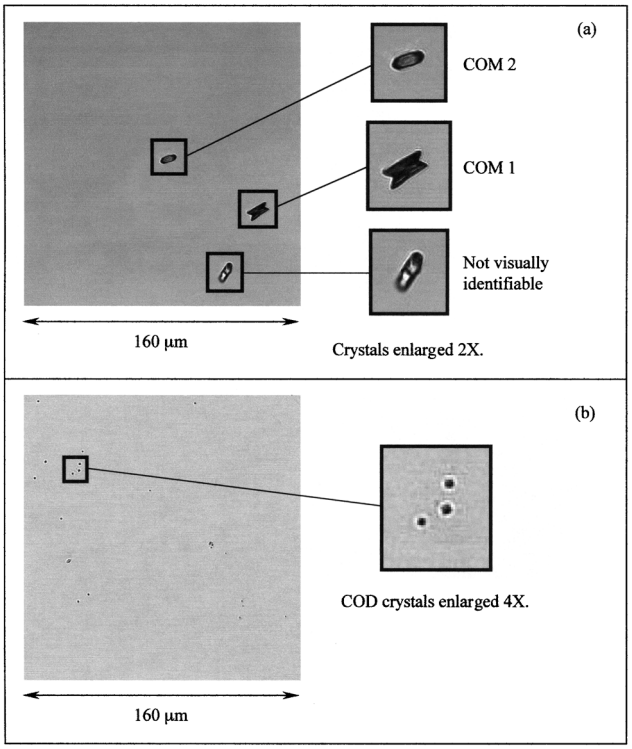

Figure 2. Images of the different calcium oxalate crystal shapes observed in the impinging-jet experiments.

(a) Crystals of the two different forms of COM are shown with a third crystal that was not visually identifiable. (b) Crystals of COD. Both images were obtained using a 40× objective and a 2× zoom. Image dimensions are 160 μm× 160 μm.

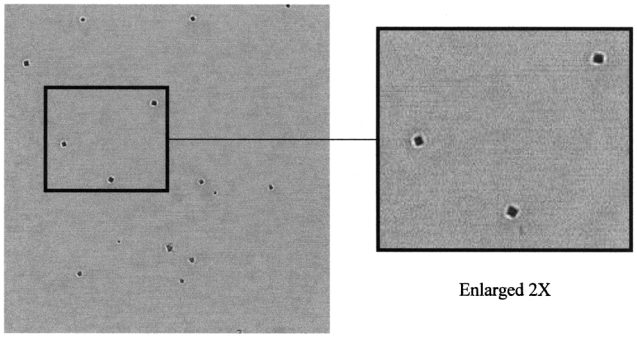

Figure 3. High magnification images of COD crystals, obtained with a 100× objective and a 2× zoom; image dimensions are 64 μm×64 μm.

Schaer et al., 1999; Rodriguez-Hornedo and Murphy, 1999). Both types of COM crystals tended to be large enough for easy identification (that is, mean dia. greater than 3 μm). Figure 2a illustrates the difference between COM1 and COM2 crystal shape. In some cases, crystals were not identifiable based on shape, and were labeled as "not visually identifiable." An example of such a crystal is also shown in Figure 2a. COD crystals tended to be smaller, often with a mean dia. less than 2 μm. The compact, square shape of the COD crystals, illustrated in Figure 2b, was distinct enough that even very small crystals, too small to identify any degree of visual detail beyond the basic outline of the crystal, could be assumed to be COD. The shape of the COD crystals imaged at 40× was verified by imaging samples with the 100× objective and a 2× zoom. The distinctive COD shape is clearly visible in Figure 3.

Within a given experiment, the means for the crystal size and number were calculated as arithmetic means. The data from multiple experiments was weighted to account for the uncertainties [standard errors (s.e.)] of the individual experiments. The weighted mean for N experiments was calculated as

$$x_{wt} = \left(\sum_{i=1}^{N} w_i x_i \right) \Big/ \sum_{i=1}^{N} w_i \tag{1}$$

where x_i represents the mean quantity for a single experiment (that is, average diameter or average number of crystals per image) and the weights w_i are the inverse squares of the corresponding uncertainties

$$w_i = 1/\text{s.e.}_i^2, \quad i = 1, 2, \ldots, N \tag{2}$$

The standard error in the weighted mean was calculated as

$$\text{s.e.}_{x_{wt}} = \left(\sum_{i=1}^{N} w_i \right)^{-1/2} \tag{3}$$

Results

Effect of quench procedure on crystallization product

An important step in the experimental procedure consisted of quenching the output from the impinging jet to reduce the supersaturation driving force, thus halting the crystal-growth process at the exit point. Without the quench step, the crystal-growth process would continue until the supersaturation was depleted to saturation. To investigate possible effects of quenching on the form of the crystallization product, crystals precipitated from equimolar calcium chloride and sodium oxalate solutions were collected into either a just-saturated quench solution or, for comparison, into an empty flask. Experiments were run with individual jet velocities of 5.3 m/s. The quenched and unquenched crystals produced from 5.0-mM reactants, the same reactant concentrations used in the remainder of this study, are shown in Figures 4a and 4b, respectively. The quenched samples consisted of single dihydrate crystals, while the crystals observed in unquenched samples contained dendrites in addition to single monohydrate crystals and a small fraction of dihydrate. Figures 4c and 4d show, respectively, the quenched and unquenched crystals produced from reactants at a slightly lower concentration of 4.0 mM. As with 5.0-mM reactants, the quenched sample produced at 4.0 mM consisted of single dihydrate crystals. The unquenched crystals formed at 4.0 mM were a mixture of monohydrate with a small amount of dihydrate.

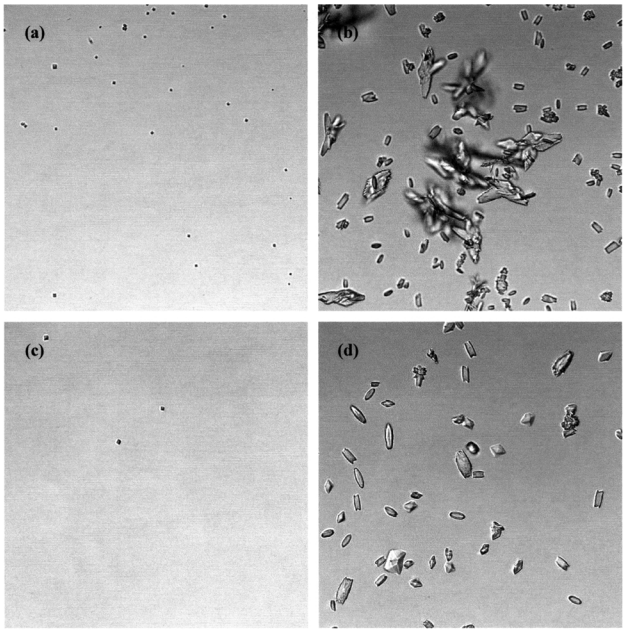

Figure 4. Quenched and unquenched samples of calcium oxalate crystals produced at 5.3-m/s jet velocity.

Samples prepared from 5.0-mM reactants and collected into (a) quench solution and (b) an empty flask (unquenched). Samples prepared from 4.0-mM reactants and collected into (c) quench solution and (d) an empty flask (unquenched). All images were obtained with a 40× objective, 2× zoom. Each image is 160 μm×160 μm.

Effect of time postjetting in quenched samples on CSD

In addition to investigating the effect of quenching, calcium oxalate crystals produced from 5.0-mM reactants were

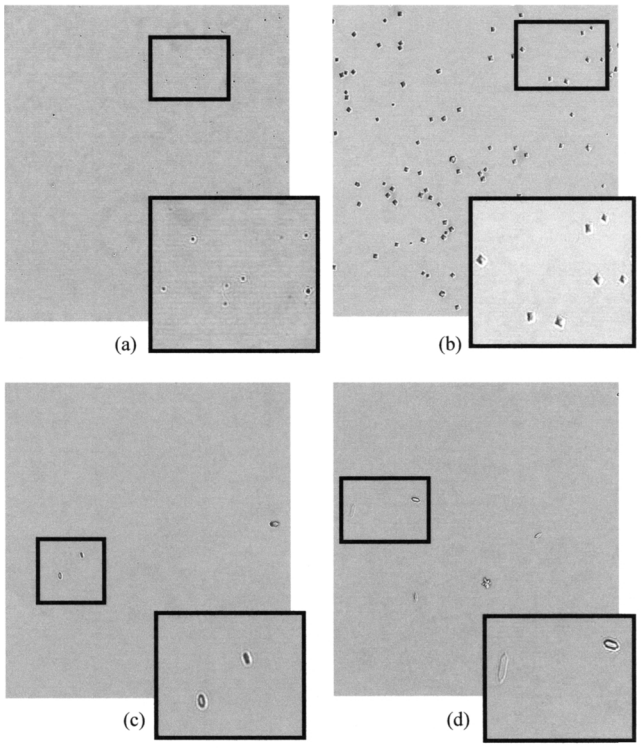

Figure 5. Calcium oxalate crystals observed at short and long times postjetting.

High linear velocity (5.8 m/s) images obtained at (a) 37-min and (b) 195-min postjetting. Low linear velocity (2.2 m/s) images obtained at (c) 36-min and (d) 105-min postjetting. All images were obtained with a 40× objective, 2× zoom. Each image is 160 μm × 160 μm.

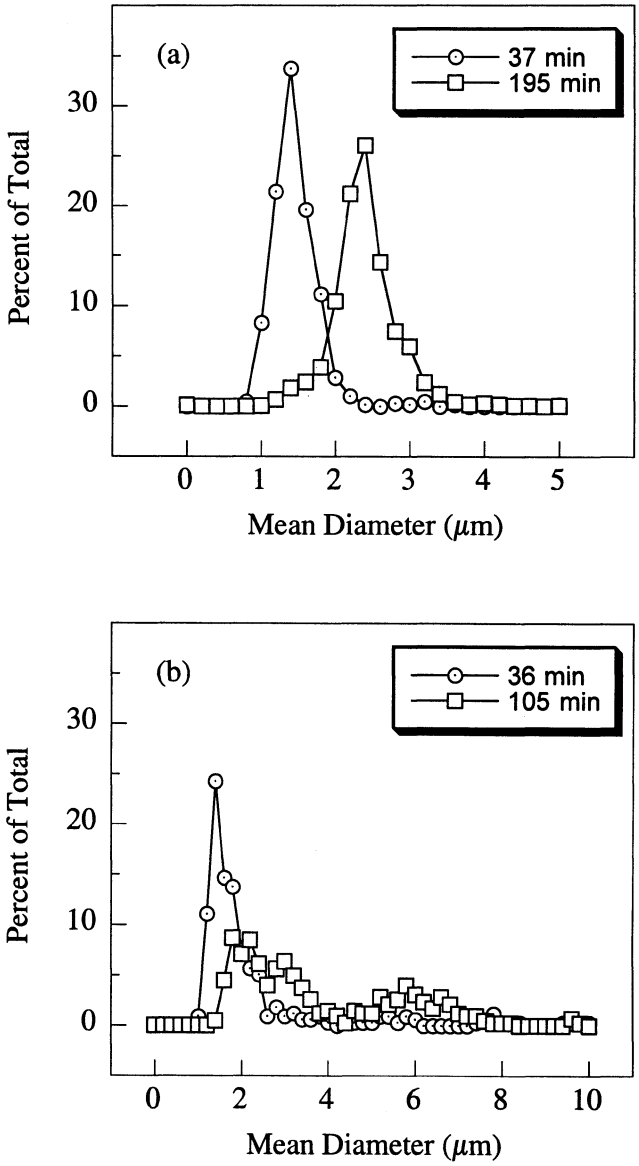

Figure 6. CSDs of calcium oxalate crystals at (a) 37-min and 195-min postjetting for high jet velocity (5.8 m/s), and (b) 36-min and 105-min postjetting for low jet velocity (2.2 m/s).

examined over a period of time following the quench step to determine whether the time delay between quenching the crystals and measuring the CSD introduced any significant changes that might affect the CSD. Over a period of 2–3 h postjetting, which was several times longer than the anticipated measurement time delay, crystals produced at both high and low jet velocity exhibited growth, as shown in Figure 5. Images of crystals produced at high jet velocity (5.8 m/s) taken at 37 min and 195 min postjetting are illustrated in Figure 5a and 5b, respectively. Images of crystals produced at low jet velocity (2.2 m/s) taken at 36 min and 105 min postjetting are illustrated in Figures 5c and 5d, respectively. The corresponding CSDs for these experiments are shown in Figure 6. During the 2.5-h time period postjetting, the mean dia. of the crystals produced at high velocity increased from 1.4 ± 0.01 μm to 2.4 ± 0.02 μm (Figure 6a) and the mean number of crystals per image increased from 27 ± 3 to 95 ± 4 (not shown). For the low-velocity experiments, the mean diameter of the crystals increased from 2.2 ± 0.12 μm to 3.7 ± 0.10 μm (Figure 6b), and the mean number of crystals per image increased from 6.7 ± 0.8 to 17.0 ± 0.9 (not shown).

The extent of crystal growth as a function of time was further evaluated within the anticipated shorter sample time range of 30–50 min postjetting. Figures 7a and 7b show the mean diameter and number of crystals per image as a function of time postjetting for five experiments performed at high linear velocity (5.3–5.8 m/s). Over this time, crystals exhibited little or no growth; the mean crystal dia. was 1.5 ± 0.01 μm. The number of crystals per image also showed little variation during this time period.

The mean dia. and number of crystals per image are shown in Figures 7c and 7d as a function of time postjetting for four experiments performed at low velocity (1.8–2.2 m/s). As with the experiments at high jet velocity, only minor variations in the crystal size and number occurred in the time range 30–50 min postjetting. Because both of these characteristics were relatively stable within the 30–50 min postjetting, subsequent measurements to investigate the effects of linear velocity on CSD were made within this time frame.

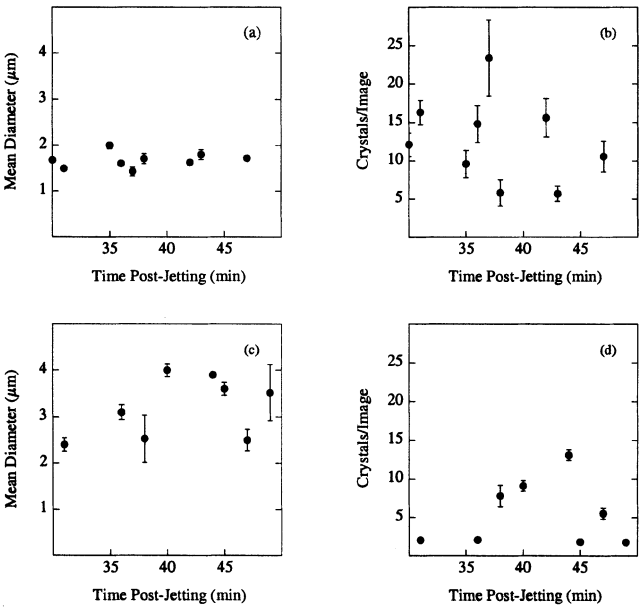

Figure 7. (a) Mean dia. and (b) number of crystals per image as a function of time postjetting for calcium oxalate crystals produced at high impinging-jet linear velocity (5.3–5.8 m/s); (c) mean dia. and (d) number of crystals per image as a function of time postjetting for calcium oxalate crystals produced at low impinging jet-linear velocity (1.8–2.2. m/s).

CSD at high linear velocity

The CSD of quenched calcium oxalate crystals produced with 5.0-mM equimolar solutions of calcium chloride and sodium oxalate at a relatively high linear velocity of 5.3−5.8 m/s varied between two main profiles, as shown in Figure 8. The crystals represented in Figure 8a were small monodisperse crystals of the metastable dihydrate form, characterized by narrow, highly reproducible distributions. The mean dia. for this set was 1.5 ± 0.01 μm, and the mean number of crystals per image was 9.4 ± 0.4. In Figure 8b, the presence of a bimodal distribution reflects the presence of both the metastable dihydrate and the larger, stable monohydrate. The second peak, representing the monohydrate, varied somewhat among the distributions shown in Figure 8b, but was present in all cases. Analysis of the variance indicated that the distributions within each group (a and b) were similar, but were not in all cases statistically equivalent (the F values for groups a and b were 17.1 and 12.6, respectively). The difference between groups a and b was much greater (the F value was 236.7) than the difference within either group. Figure 8c shows the average CSD for the two basic CSDs illustrated in Figures 8a and 8b. Table 1 summarizes the corresponding weighted number and weighted mean dia. of crystals and the fraction of monohydrate.

These experiments were run over a period of seven months, beginning in January and ending in July. The CSD profiles exhibited a stochastic variability that, surprisingly, appeared to correlate to some extent with the date of the experiment, as shown in Figure 9, indicating the trend observed as a function of the chronological sequence of experimental runs. The

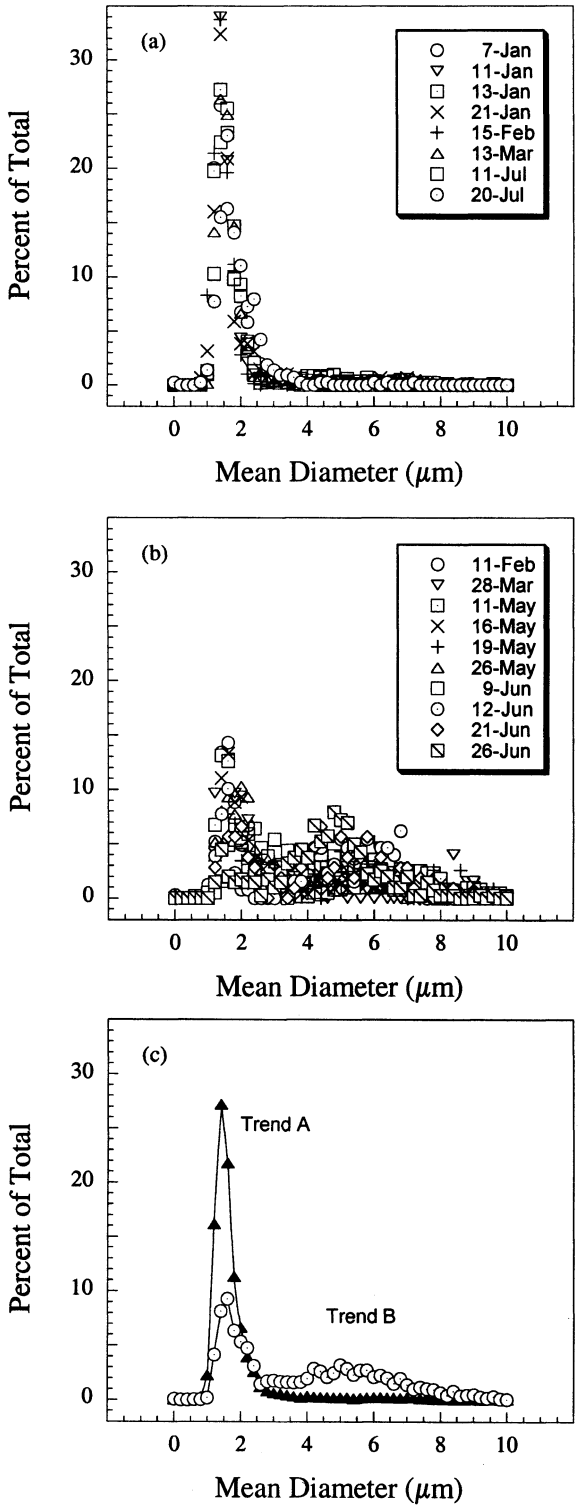

Figure 8. Characteristic CSDs for calcium oxalate crystals produced under identical conditions at high linear velocity (5.3–5.8 m/s).

(a) Single peak at 1.5 μm; (b) bimodal distribution with a peak at 1.8 μm and a second peak at 6 μm; (c) average CSD for each of the trends shown in (a) and (b). The peak observed in both (a) and (b) at less than 2 μm results from a population of dihydrate crystals. The second peak in (b) results from the appearance of a population of monohydrate crystals.

Table 1. Crystal Number and Size Corresponding to Each of the CSD Trends

Trend	Total Number of Crystals*	Number of Crystals/ Image ± S.E.**	Mean Dia. ± S.E. (μm)	% COM ± S.E.
Figure 8a	6,536	9.4 ± 0.4	1.53 ± 0.01	~ 0
Figure 8b	2,727	3.5 ± 0.2	3.85 ± 0.07	36 ± 3

*Sum of all crystals counted in all experiments corresponding to a given trend.
**Weighted mean number of crystals counted in an individual image. For example, Figure 8a was constructed from 525 images containing a total of 6,536 crystals with a weighted average of 9.4 crystals per image.

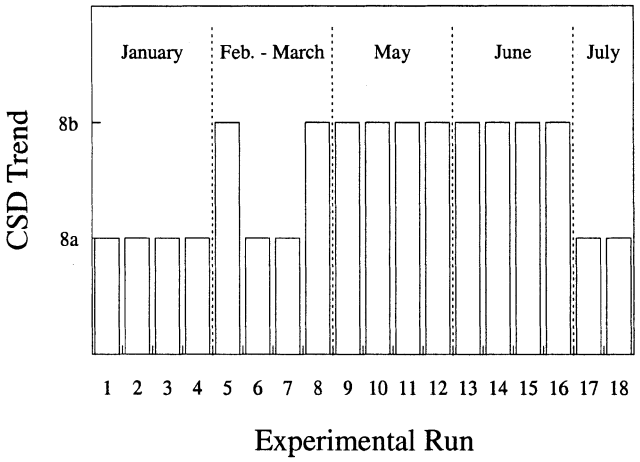

Figure 9. CSD trend observed for calcium oxalate produced at high linear velocity (5.3–5.8 m/s) as a function of the experimental run sequence.

Experiments were run over a seven-month time period, as indicated along the upper *x*-axis. The CSD trend shown on the *y*-axis indicates which of the two characteristic CSDs shown in Figures 8a and 8b was produced by a given experiment. For example, in Feb./March the first experiment fit trend 8b, and the second and third fit trend 8a.

monodisperse distributions represented in Figure 8a occurred during the first three-month period and again in the last month, but were not observed in the interim four months. During the middle three-month period, the distributions, although somewhat variable, were all bimodal distributions.

CSD at low linear velocity

The average CSD for crystals formed in four experiments at low jet velocity (1.8–2.2 m/s) is shown in Figure 10a. In all experiments, the crystal samples were quenched and images were obtained within 30–50 min postjetting. The mean crystal dia. was 3.4 ± 0.05 μm, and the average number of crystals per image was 2.2 ± 0.10. The average CSD for crystals formed at high jet velocity (5.5–5.8 m/s) during the same time period is shown for comparison in Figure 10b. In addition to having a larger mean diameter, the crystals at the lower velocity had fewer crystals per image, only 2.2 ± 0.10 vs. 13.9 ± 0.63 for those produced at the higher velocity.

Calcium depletion in jet

The reduction in supersaturation was estimated by measuring the calcium concentration in the jetted solution. At high

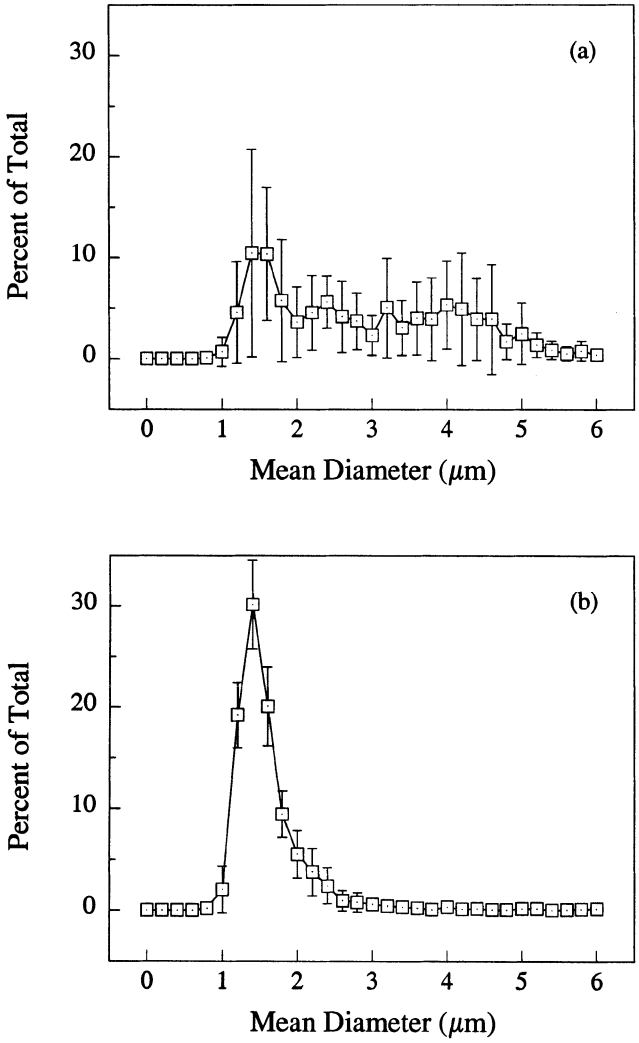

Figure 10. Average CSD for calcium oxalate crystals produced during a three-month time period at (a) low linear velocity (2.2 m/s), and (b) high linear velocity (5.8 m/s).

linear velocity, the average calcium concentration in the solution exiting the jet was 0.90 ± 0.1 mM, indicating a 64% reduction in calcium (from 2.5 mM). At low linear velocity, the average calcium concentration in the material exiting the jet was 1.05 ± 0.35 mM, indicating a 58% reduction in calcium. Although this is not a statistically significant difference, we expect that more calcium is depleted in the jet at high velocity than at low velocity through nucleation, but that calcium

depletion by crystal growth decreases the difference by the time the calcium is measured. Crystal growth obscures differences in the amount of calcium consumed by nucleation and calcium consumed by growth.

Discussion

The impinging-jet mixer is a potentially useful device for the direct production of small, monodisperse crystals in rapidly nucleating systems. The ability to produce crystals with these characteristics can be particularly important for pharmaceutical compounds where high crystal surface area is required for drug bioavailability and a narrow and reproducible size distribution contributes to improved processability and consistent product performance. Midler et al. (1994) have described the use of the impinging jet for forming small, monodisperse crystals of pharmaceutical compounds, but much remains to be understood about the process before its usefulness as a production method can be fully evaluated. In this work, we have focused on the impinging-jet crystallization of a single model system, calcium oxalate, in an effort to further characterize the process and key factors that affect it. Our results support the claim that small crystals can be produced in the jet. However, the CSD varied somewhat between runs, an effect we believe can be attributed to a combination of crystallization kinetics and the mixing characteristics of the jet. The size and number density of the crystals produced also appeared to be influenced by the impinging-jet linear velocity.

Variability in the CSD

Crystal sizes ranged from 1.5 μm to 4.4 μm for individual jet velocities in the range of 5.3–5.8 m/s, the primary condition we tested. Crystals of this size are highly desirable for many pharmaceutical compounds to meet high bioavailability and short dissolution time requirements, but generally cannot be produced using a conventional crystallizer without a postcrystallization milling step (Midler et al., 1994). In addition to a small mean size, a narrow size distribution with a reproducible shape is desirable for product uniformity and to facilitate ease of postcrystallization processing and formulation. Although the CSDs we observed were relatively narrow, their shape varied, primarily due to the formation of differing ratios of two hydrates of calcium oxalate despite presumably identical experimental conditions. As reflected by the CSDs in Figure 8, a single, major peak appeared at the lower end of the size scale for runs in which COD predominated. A shift of the CSD to the right and the appearance of a second peak at the higher end of the size scale corresponded to an increasing presence of COM. Much smaller variations in the CSD occurred when either the COD or the COM hydrate form dominated, likely reflecting a degree of growth-rate dispersion and/or size-dependent growth in the system (Tavare, 1995). There are at least two factors that we believe contributed to the variations in hydrate ratio: (1) imperfect mixing in the jet, and (2) the balance between kinetics and thermodynamics in the system.

Process conditions that favor the formation of COD differ from those favoring COM. COM is the thermodynamically more stable form, but according to Ostwald's step rule it has the lowest reaction rate (Brecevic et al., 1986). The crystal form lying nearest in free energy to the original supersaturated state has the highest reaction rate, but is not necessarily the most thermodynamically stable form (Grant, 1999). At high levels of supersaturation (that is, high departures from equilibrium), the nucleation of calcium oxalate is kinetically controlled (Bretherton and Rodgers, 1998; Garside et al., 1982) and the favored crystal hydrate form would be the metastable dihydrate.

Incomplete mixing in the jet could effectively alter the supersaturation, and, thus, the favored hydrate form. The initial mixing in the impinging jet occurs in the impingement plane, a relatively small volume, which leads to increased contact area between the reactant streams and faster micromixing than in a conventional stirred tank. Under ideal mixing conditions of high velocity, equal jet momentum, and perfectly aligned jets, the collision between the reactant streams results in a large energy dissipation in the impingement zone and rapid mixing on a molecular scale (Demyanovich and Bourne, 1989). This rapid micromixing of the reactant streams leads to the creation of a high level of supersaturation and should favor the COD crystal form. In the case of imperfectly aligned jets, less energy is dissipated by mixing, causing a lower effective supersaturation that would favor the COM. In our experiments we observed that the impingement plane oscillated slightly from right to left under normal operation, indicating an instability in the system and introducing the possibility of variable mixing, even for identical system temperature, flow rate, and reactant concentrations. Experiments in which the impinging reactant streams were fluorescently dyed suggest that differences in local concentrations do result from the minor variations in plane orientation that constitute these oscillations, and that the hydrate form can be correlated to the local concentration differences. These results will be presented in a subsequent article.

Given the relatively high level of supersaturation in our experiments, the crystal nucleation process was most likely kinetically controlled, favoring COD formation in well-mixed solutions. However, decreased mixedness due to deflection of the reactant streams could create regions of lower supersaturation in which COM would preferentially form. In addition, thermodynamic influences such as Ostwald ripening could have played a role in the quench step following jetting. Ostwald ripening is a phenomenon in which the smallest crystals dissolve, thus providing additional supersaturation that enables further growth of the slightly larger crystals (Dirksen and Ring, 1991). The effects of Ostwald ripening could be significant for a population of crystals containing both COM and COD, because the COD crystals are less thermodynamically stable and would therefore dissolve faster, causing a shift in the hydrate distribution with time.

Although the preceding arguments provide at least a plausible explanation for the variable hydrate ratio that we observed, they do not explain the slight time dependence in the results suggested by Figure 9. One factor that may have contributed is impurity buildup due to a reaction between the stainless steel system and the chloride ions, which could change the nucleation kinetics, making the system more sensitive to mixing. Another possibility is that the jet nozzles shifted position slightly over time, making the mixing less

ideal. This could help to explain why COD reappeared as the predominant hydrate form after a number of runs, yielding a large fraction of COM. The jet nozzles may simply have shifted back into their original position after a period of time. If such shifts occurred, they were too subtle to be detected by careful visual scrutiny and would have been the result of ambient mechanical or thermal fluctuations in the laboratory.

The fact that different hydrate ratios were obtained at identical system conditions suggests that we were operating within a critical region of the parameter space in which the system was very sensitive to minor variations. It is possible that the system would behave more reliably under different operating conditions. However, in various changes we made to the operating conditions, we were unable to produce a less variable hydrate ratio while maintaining the desired product characteristics (Condon, 2001). For example, in experiments conducted with 3.5-mM reactants, only COM formed in significant amounts, but the crystals were larger, ranging from 4.0 μm to 6.0 μm in dia.

Effect of linear velocity on the CSD

In addition to the experiments performed at high linear velocity (5.3–5.8 m/s), a limited number of experiments were performed at a lower velocity of 1.8–2.2 m/s. When compared to the complete data set at high velocity, the results at low velocity are not significantly different. However, a significant difference does exist if we consider only the high-velocity experiments performed over the same time period as the low-velocity experiments, that is, during the first three months (Figure 9). This comparison is particularly reasonable if the preceding arguments regarding the time variable behavior of the system on the scale of months are assumed to be valid. During the initial three-month period, the CSD at high velocity was especially reproducible, suggesting that any unintended changes in the system were minimal. The series of crystallization experiments performed in the impinging jet at high linear velocity during this initial time period yielded a greater total number of crystals with a smaller average size than those produced at lower velocities (Figure 10a and 10b). The CSD data for the high-velocity experiments in the time frame considered is significantly more consistent among the different experiments than the low-velocity experiments. Subsequent variability in the high-velocity experiments limits the certainty with which we can conclude that calcium oxalate crystallization is affected by jet velocity. However, our results are consistent with Mahajan and Kirwan (1996), who found that when the mixing time was faster than the nucleation time, the mean crystal size was smaller and the distribution of sizes was narrower for the drug Lovastatin in a nonsubmerged impinging-jet system.

Several other authors have reported on the relationship between mixing and CSD, and it is generally accepted that micromixing effects can be significant for processes with fast nonlinear kinetics such as primary nucleation (Liszi et al., 1997; Manth et al., 1996; Franke and Mersmann, 1995; Garside, 1985). Franke and Mersmann (1995) demonstrated that the nucleation rate increases with power input due to accelerated micromixing processes in MSMPR and batch crystallizers. When the mixing time is faster than the reaction time, a homogeneous environment is created prior to nucleation and maximum supersaturation is achieved, resulting in a high nucleation rate and the creation of a large number of small particles. If the mixing time is longer than the reaction time, concentration gradients can exist and lower the effective supersaturation, leading to a lower overall nucleation rate and the production of fewer crystals with a larger average size.

The dependence of the CSD on the impinging-jet linear velocity could be an indication that the nucleation rate is mixing controlled, although it is difficult to be certain, because the results are complicated by the presence of multiple hydrates. If a single-crystal form develops, the differences in CSD can be attributed solely to variations in the local supersaturation. However, with a multiple hydrate (or polymorph) system, differences in supersaturation can affect the crystal form produced as well as the CSD. At high impingement velocity (that is, good mixing and high supersaturation levels), the metastable COD form is preferred, while the COM is favored at low velocities (that is, poor mixing and low supersaturation). Because changing reactant stream velocity alters the degree of mixedness (and, hence, nucleation and growth rates), leading to changes in the crystal form (which have different solubilities and growth rates), it becomes impossible to separate the CSD effects due simply to increasing-jet velocities from those due to a change in the preferred hydrate form. However, additional experiments performed with 3.5-mM reactant solutions, a concentration where only the stable monohydrate crystals formed in significant amounts, also indicated that the crystal size decreased and the crystal number increased with increasing linear velocity. This trend is consistent with an increase in velocity accelerating the micromixing process, and thereby increasing the nucleation rate and lowering the average crystal size.

Effect of quenching

The comparison between quenched and unquenched samples clearly demonstrates that the quench step was effective in stopping, or at least significantly slowing, the crystallization process. The difference between quenched and unquenched crystals can be considered simply as in increase in the time period postjetting that the crystallization is allowed to proceed. The quench step stops the crystallization process by diluting the solution to its equilibrium concentration. Without the quench, crystallization continues until the reactants are depleted to their equilibrium level. The outlet tubing length between the impinging jet and the quench solution was adjusted to maintain a residence time of 5–6 s prior to quench, effectively stopping the crystallization 5–6 s postjetting.

The effect of quenching was investigated at two different reactant concentrations, 4.0 and 5.0 mM. As illustrated in Figures 4a and 4c, respectively, with 4.0 and 5.0 mM reactant concentrations, only dihydrate crystals were observed in the quenched samples. At high supersaturation, dihydrate is kinetically favored and will form faster than the thermodynamically stable monohydrate (Finlayson, 1978). The fact that only dihydrate crystals were present in the quenched samples suggests that monohydrate had not nucleated or grown to a stable size before the solution was quenched. This observation indicates that the induction time, the time between the creation of supersaturation and the formation and growth of the nuclei to a stable size, for monohydrate is longer than 5 s at 4.0 and 5.0 mM. The higher number of dihydrate crystals ob-

served at 5.0 mM is consistent with an expected increase in the nucleation rate at a higher reactant concentration. The unquenched samples from 4.0- and 5.0-mM reactant concentrations, shown in Figures 4b and 4d, respectively, contained both monohydrate and dihydrate with the samples from 5.0 mM also containing dendrites. The appearance of the slower-forming monohydrate was presumably due to the fact that, in the absence of quenching, crystal growth was able to continue for a much longer period of time (>10 min, as compared to 5–6 s for quenched samples). Dendrite crystals, often described as having treelike structures (Nyvlt, 1971), form due to mass-transport limitations or "traffic" at the crystal surface under fast growth conditions (Walton, 1967; Cody and Cody, 1995). If the solvent molecules cannot diffuse away from the surface quickly enough, they block the normally fast-growing surfaces. However, corners are less severely blocked than surfaces and continue to grow unimpeded by diffusion limitations, leading to dendrite structures. As with the quenched samples, the number of crystals appeared to increase with increasing concentration.

Effect of postjetting time for quenched samples

One challenge in studying crystallization in the impinging jet is isolating the effects of the impinging jet on nucleation rates from subsequent growth and/or dissolution during the observation period. To minimize changes in the product after exiting the jet, the jetted solution was collected into a just-saturated calcium oxalate quench solution. With ideal mixing in the jet, supersaturation in the jetted solution would be depleted to the saturation (equilibrium) value, and no further nucleation, growth, or dissolution of the crystals would occur in the quench solution. Although measurements of unreacted calcium in the jet output confirmed that the jet was effective in relieving the supersaturation, reducing it by 60% or more, it remained sufficiently high to promote some postjetting behavior, as indicated by the changes observed in crystal number and size after several hours in the quench solution (Figure 5). Based on the degree of supersaturation, these changes were most likely due to the growth of existing crystals. In our experiments, the jetted solution was collected into the quench solution at a volume ratio of 1:3.3. This dilution would bring the concentration in the quench solution to approximately twice the solubility of COM and 1.3 times the solubility of COD. With a high percentage of the supersaturation depleted in the impinging jet and the dilution into the quench solution, it is unlikely that the level of supersaturation was high enough to promote the nucleation of new crystals. Therefore, the undepleted supersaturation from the jet was probably not high enough to promote the nucleation of new crystals once quenched, but rather, contributed to the growth of existing crystals. The increase in the number of crystals at postjetting times more than 100 min, as seen in Figure 5, was most likely due to small crystals growing to a size where they became visible rather than to the formation of new crystals.

Ostwald ripening could have contributed to changes in the CSD with time in the quench solution. Ostwald ripening is a common phenomenon in precipitation processes in which larger crystals grow at the expense of smaller crystals (Franke and Mersmann, 1995). In addition, larger crystals generally grow faster because crystal-growth rate is proportional to surface area. Stochastic variation in the growth rate may occur, as well (Tavare, 1995). The changes in CSD at successive times are likely due to a combination of Ostwald ripening, size-dependent growth, and growth-rate dispersion. In practice, it is difficult to separate the influences of size-dependent growth and growth-rate dispersion, which may occur concurrently (Mersmann, 1995; Tavare, 1995). A wide CSD tends to become even more exaggerated with time due to size-dependent growth, whereas an initially monodisperse population is likely to remain monodisperse. At high supersaturation, classic nucleation theory predicts rapid, almost instantaneous formation of nuclei, which then undergo crystal growth with continued depletion of supersaturation. Thus, homogenous nucleation would be expected to produce a monodisperse distribution of crystal sizes (Bhandarkar et al., 1989). For the experiments performed at high velocity, a narrow CSD is observed, even after long times (Figure 6a), suggesting homogeneous nucleation. At lower velocity (Figure 6b), the change in CSD over time suggests that the initial population of crystals was not monodisperse, and was possibly the result of a combination of homogenous and heterogeneous nucleation. This would be consistent with the slower velocity leading to concentration gradients and a wider CSD, as discussed earlier.

Summary

The impinging jet operated in nonsubmerged mode was used to produce small, monodisperse crystals of calcium oxalate from calcium chloride and sodium oxalate at equimolar reactant concentrations of 5.0 mM. However, the results were complicated by the presence of two different hydrate forms. At high linear velocity (5.3–5.8 m/s), CSDs varied between a unimodal CSD representing metastable dihydrate crystals and a bimodal CSD, with one peak representing dihydrate and the other corresponding to monohydrate crystals. Additional experiments performed at a lower linear velocity suggested a dependence of CSD on jet velocity, but a definitive correlation could not be made due to the formation of multiple hydrates, and, thus, variable CSDs at the high linear velocity. The variation in hydrate ratio between runs at identical conditions suggests a level of sensitivity in the system that could lead to difficulty in its application. The relationship between mixing in the impinging jet and hydrate distribution will be further examined in a future article.

Acknowledgments

This work was partially supported by funding from the New Jersey Commission on Science and Technology. The authors thank Art Andrews, Mike Midler, and Fernando Muzzio for helpful discussions.

Literature Cited

Benet, N., L. Falk, H. Murh, and E. Plasari, "Experimental Study of a Two-Impinging Jet Mixing Device for Application in Precipitation Processes," *Ind. Cryst.*, 1 (1999).

Bhandarkar, S., R. Brown, and J. Estrin, "Studies in Rapid Precipitation of Hydroxides of Calcium and Magnesium," *J. Cryst. Growth*, **97**, 406 (1989).

Brecevic, L., D. Skrtic, and J. Garside, "Transformation of Calcium Oxalate Hydrates," *J. Cryst. Growth*, **74**, 399 (1986).

Bretherton, T., and A. Rodgers, "Crystallization of Calcium Oxalate in Minimally Diluted Urine," *J. Cryst. Growth*, **192**, 448 (1998).

Cody, A., and R. Cody, "Dendrite Formation by Apparent Repeated Twinning of Calcium Oxalate Dihydrate," *J. Cryst. Growth*, **151**, 369 (1995).
Condon, J. M., "Investigation of Impinging Jet Crystallization with a Calcium Oxalate Model System," PhD Thesis, Rutgers University, Piscataway, NJ (2001).
Demyanovich, R. J., and J. R. Bourne, "Rapid Micromixing by the Impingement of Thin Liquid Sheets. 1. A Photographic Study of the Flow Pattern," *Ind. Eng. Chem. Res.*, **28**, 825 (1989).
Dirksen, J. A., and T. A. Ring, "Fundamentals of Crystallization: Kinetic Effects on Particle Size Distributions and Morphology," *Chem. Eng. Sci.*, **46**(10), 2389 (1991).
Dunitz, J., and J. Bernstein, "Disappearing Polymorphs," *Acc. Chem. Res.*, **28**, 193 (1995).
Finlayson, B., "Physicochemical Aspects of Urolithiasis," *Kidney Int.*, **13**, 344 (1978).
Franke, J., and A. Mersmann, "The Influence of the Operational Conditions on the Precipitation Process," *Chem. Eng. Sci.*, **50**(11), 1737 (1995).
Garside, J., "Tailoring Crystal Products in Precipitation Processes and the Role of Mixing," *AIChE Symp. Ser.*, **284**(87), 16 (1991).
Garside, J., "Industrial Crystallization from Solution," *Chem. Eng. Sci.*, **40**, 3 (1985).
Garside, J., L. Brecevic, and J. W. Mullin, "The Effect of Temperature on the Precipitation of Calcium Oxalate," *J. Cryst. Growth*, **57**, 230 (1982).
Grant, D., *Theory and Origin of Polymorphism, in Polymorphism in Pharmaceutical Solids*, Dekker, New York (1999).
Liszi, M., M. Hasznos-Nezdei, and B. Farkas, "Effect of Mixing on Primary Nucleation," *Hung. J. Ind. Chem.*, **25**, 181 (1997).
Mahajan, A. J., and D. J. Kirwan, "Micromixing Effects in a Two-Impinging Jets Precipitator," *AIChE J.*, **42**, 1801 (1996).
Manth, T., D. Mignon, and H. Offermann, "The Role of Hydrodynamics in Precipitation," *J. Cryst. Growth*, **166**, 998 (1996).
McCauley, J., "Detection and Characterization of Polymorphism in the Pharmaceutical Industry," *AIChE Symp. Ser.*, **284**(87), 16 (1991).
Mersmann, A., *Fundamentals of Crystallization, in Crystallization Technology Handbook*, Dekker, New York (1995).
Midler, M., E. Paul, E. Whittington, M. Futran, P. Liu, J. Hsu, and S. Pan, "Crystallization Method to Improve Crystal Structure and Size," U.S. Patent No. 5,314,506 (1994).
Nyvlt, J., *Industrial Crystallization from Solutions*, Butterworths, London (1971).
Rodriguez-Hornedo, N., and D. Murphy, "Significance of Controlling Crystallization Mechanisms and Kinetics in Pharmaceutical Systems," *J. Pharm. Sci.*, **88**(7), 651 (1999).
Schaer, E., P. Guichardon, L. Falk, and E. Plasari, "Determination of Local Energy Dissipation Rates in Impinging Jets by a Chemical Reaction Method," *Chem. Eng. J.*, **72**, 125 (1999).
Shekunov, B. Y., and P. York, "Crystallization Processes in Pharmaceutical Technology and Drug Delivery Design," *J. Cryst. Growth*, **211**, 122 (2000).
Skrtic, D., M. Markovic, L. Komunjer, and H. Furedi-Milhofer, "Precipitation of Calcium Oxalates from High Ionic Strength Solutions. I. Kinetics of Spontaneous Precipitation of Calcium Oxalate Trihydrate," *J. Cryst. Growth*, **66**, 431 (1984).
Tavare, N., "Continuous Crystallization," Industrial Crystallization, Process Simulation Analysis and Design, D. Luss, ed., Plenum Press, New York (1995).
Van Leeuwen, M. L. J., O. S. L. Bruinsma, and G. M. van Rosmalen, "Three-Zone Approach for Precipitation of Barium Sulphate," *J. Cryst. Growth*, **166**, 1004 (1996).
Walton, A., *The Formation and Properties of Precipitates, Chemical Analysis*, Wiley, New York (1967).

Manuscript received July 18, 2002, revision received Jan. 3, 2003, and final revision received May 19, 2003.